Electronic Supplementary Material (ESI) for Catalysis Science & Technology

Effect of g-C3N4 loading in TiO2 – based Photocatalysts: UV and Visible degradation of Toluene

M.J. Muñoz-Batista,[a] A. Kubacka,[a,*] and M. Fernández-García[a,*]

Quantum yield calculation

To evaluate the Quantum yields, it is necessary to know the local superficial rate of photon absorption ($e^{a,s}$). At each ($x,y,z \equiv Xs,Ys,Zs$) position on the catalytic film the local superficial rate of photon absorption can be determined from Equation (1).

$$e_{\lambda}^{a,s}(x,y,z) = \sum_{L=1}^{L=4}\sum_{\lambda}\int_{\varphi_{min}}^{\varphi_{max}}\int_{\Theta_{min}}^{\Theta_{max}} I_{\lambda,L} \times \exp\left(-\frac{K_{\lambda,g}e_g}{\cos\beta}\right)\left[1 - exp\left(\frac{K_{\lambda,s}e_s}{\cos\beta}\right)\right]sin^2\varphi\ \left[\left(\frac{X_s - X_L}{R}\right)\cos\Theta + \left(\frac{X_s}{R}\right)sin\Theta\right]d\varphi d\Theta + \sum_{L=1}^{L=4}\sum_{\lambda}\int_{\varphi}$$

1

The integration limits for the spherical coordinates φ and Θ can be evaluated taking into account: (i) the coordinate system adopted (Figure S1), (ii) the geometry/dimensions and characteristics of the reactor and the lamp (Figure S2 and Table S1) and are given by Equations 2-5.

$$\varphi_{mín} = \tan^{-1}\left(\frac{X_L - Xs}{Y_L - Ys}\right) - \sin^{-1}\left(\frac{RL}{(X_L - Xs)^2 + (Y_L - Ys)^2}\right)$$

2

$$\varphi_{max} = \tan^{-1}\left(\frac{X_L - Xs}{Y_L - Ys}\right) + \sin^{-1}\left(\frac{RL}{(X_L - Xs)^2 + (Y_L - Ys)^2}\right)$$

3

$$\Theta_{mín}(\varphi) = \cos^{-1}\frac{-Zs}{(X_{Lm}(\varphi) - Xs)^2 + (Y_{Lm}(\varphi) - Ys)^2 + Zs^2}$$

4

$$\Theta_{max}(\varphi) = \cos^{-1}\frac{ZL - Zs}{(X_{Lm}(\varphi) - Xs)^2 + (Y_{Lm}(\varphi) - Ys)^2 + Zs^{22}}$$

5

Where:

$$X_{Lm}(\varphi) = X_L + (Xs - Y_L)\cos\varphi^2 + (Y_L - Ys)(\cos\varphi \operatorname{sen}\varphi) - \operatorname{sen}\varphi\sqrt{(RL^2 - (Xs - X_L)\cos\varphi + (Y_L - Ys)\operatorname{sen}\varphi)^2)} \quad 6$$

$$Y_{Lm}(\varphi) = Ys_i + (Y_L - Ys)\cos\varphi^2 + (Xs - X_L)(\cos\varphi \operatorname{sen}\varphi) - \cos\varphi\sqrt{(RL^2 - (Xs - X_L)\cos\varphi + (Y_L - Ys)\operatorname{sen}\varphi)^2)} \quad 7$$

Values of $K_{\lambda,g}e_g$ (glass) and $K_{\lambda,s}e_s$ (for each sample), were determined from spectral transmittance measurements (Figure S3). Note that each point the $e^{a,s}$ was obtained take into account the direct and indirect radiation fluxes, as is schematically shown in Figure S4. (see ref. 23 of the main paper for details).

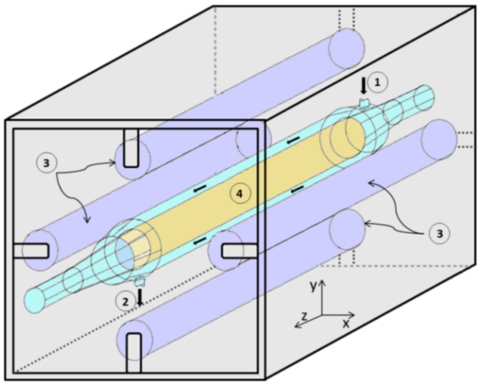

Figure S1. (A) Photocatalytic annular reactor. (1) gas inlet, (2) gas outlet, (3) lamps, (4) catalyst sample.

Table S1. Reactor and lamps characteristics

Lamp length (cm)	19
Lamp radius (cm)	0.8
UV/Sunlight Nominal power (W)	6
Reactor length (cm)	15
Reactor Inner radius (cm)	0.8
Reactor Outer radius (cm)	1.2

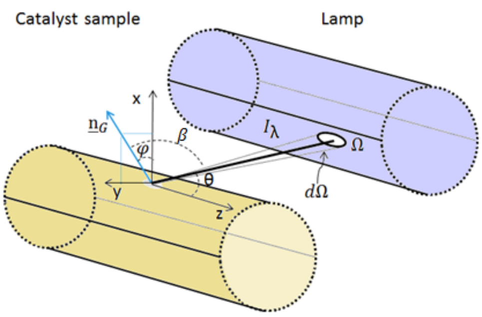

Figure S2. Coordinate system used.

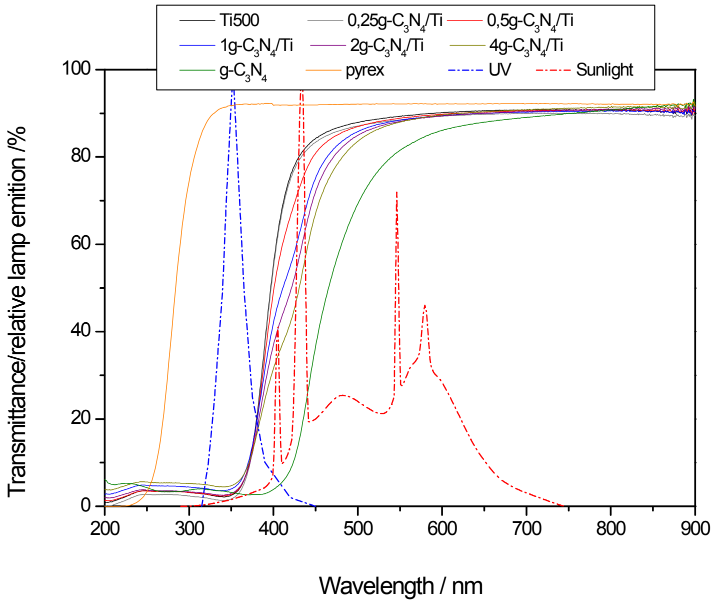

Figure S3. Transmittance of pyrex, samples and Intensity distribution of the UV and sunlight-type lamp.

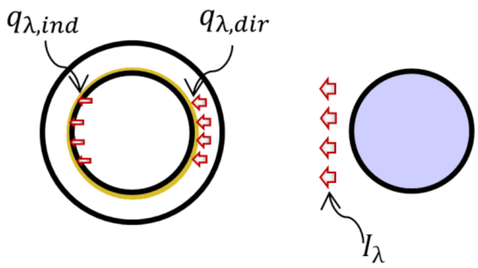

Figure S4. Radiation fluxes scheme on the sample film.

Nomenclature

$e^{a,s}$: local rate of photon absorption, Einstein cm^{-2} s^{-1}

q: local net radiation flux (W cm^{-2})

I: lamp radiation intensity, Einstein cm^{-2} s^{-1}

K: spectral absorption coefficients, dimensionless

e: thickness, cm

x,y,z: cartesian coordinate, cm

φ,Θ: spherical coordinate, rad

$\underline{n_G}$: outwardly directed (to the catalytic film) unit normal vector, dimensionless

Ω: solid angle, sr

$\underline{\Omega}$: unit vector in the direction of radiation propagation, dimensionless

β : angle between the ray trajectory and the film outwardly directed normal, rad

λ: wavelength, nm

R: reactor radius, cm

RL: lamp radius, cm

Subscripts

g: relative to glass

s: relative to the sample film

ind: relative to the indirect net radiative flux

dir: relative to the direct net radiative flux

max: maximum limiting value

min: minimum limiting value

L: relative to lamp

s: relative to the sample film

Lm: relative to the surface lamp

Photoluminescence data

In Fig. S5 we compare the photoluminescence spectra of selected samples and the corresponding to a physical mixture of their components. The larger intensity of the real vs. ideal systems suggests the existence of de-excitation path(s) not present in the parent materials as a result of the interaction between components.

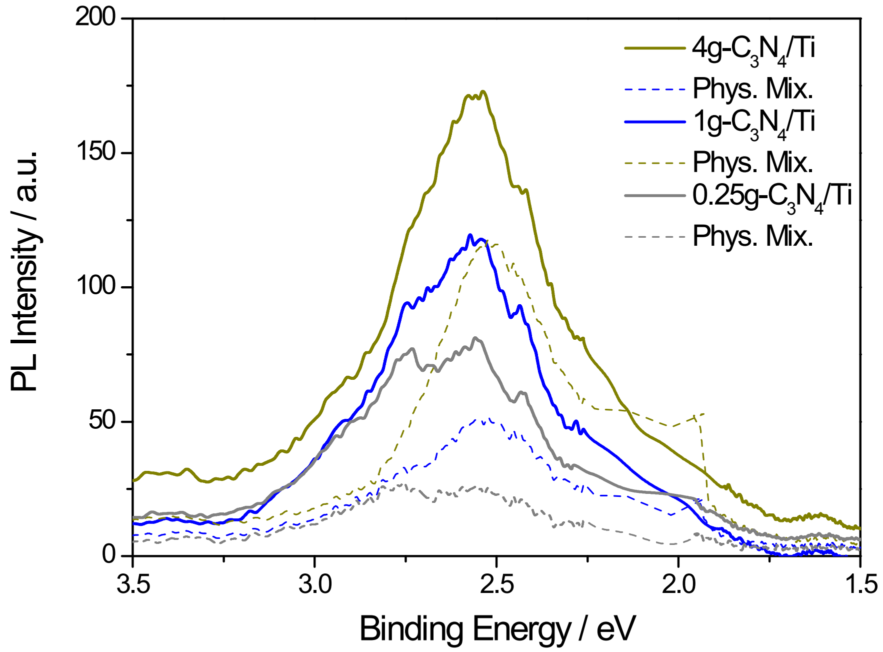

Figure S5. Photoluminescence spectra for selected samples and corresponding physical mixtures under 280 nm excitation.